



Client:

SKB

Report No.: R12-019 – Version 3

Project Title:

Residual stress measurements within the Nodular Cast Iron PWR Insert of a
radioactive waste canister

Author:

Dr. E. Kingston

13th November 2013

CONTENTS

| | | |
|-----------|---|-----------|
| 1 | INTRODUCTION..... | 3 |
| 2 | SPECIMEN DESIGN | 3 |
| 3 | INCREMENTAL CENTRE-HOLE DRILLING PROCEDURE | 3 |
| 4 | DEEP-HOLE DRILLING PROCEDURE | 4 |
| 5 | MEASUREMENT LOCATIONS | 6 |
| 6 | RESULTS AND DISCUSSION | 7 |
| 7 | CONCLUSIONS..... | 10 |
| 8 | REFERENCES | 10 |
| 9 | TABLES | 11 |
| 10 | FIGURES | 19 |

| | |
|---|-----------|
| <i>Figure 1: Technical drawing of the complete Cast Iron Insert showing the section measured by VEQTER and the location of the inserted plates at 800 mm separation. All dimensions given in mm. Annotations in red given as updates to the original CAD drawing provided to reflect the work finally carried out.</i> | <i>19</i> |
| <i>Figure 2: Photograph of the Cast Iron Insert section supplied for measurement with ICHD strain gauges attached by VEQTER.....</i> | <i>20</i> |
| <i>Figure 3: A photograph of the SGR attached at location ICHD3 with axes notation shown.</i> | <i>20</i> |
| <i>Figure 4: A photograph of the ICHD setup during the measurement process.....</i> | <i>21</i> |
| <i>Figure 5: A schematic of the five stages involved in the standard DHD procedure for a welded component.....</i> | <i>21</i> |
| <i>Figure 6: A technical drawing of the complete Cast Iron Insert with annotated section measured and measurement locations. All dimensions given in mm.</i> | <i>22</i> |
| <i>Figure 7: Photographs of the ICHD and DHD measurements being carried out at location 1.</i> | <i>23</i> |
| <i>Figure 8: A photograph of the air gauge diameter measurement process being carried out at DHD2.</i> | <i>24</i> |
| <i>Figure 9: Photographs of the ICHD and DHD measurements being carried out at location 3.</i> | <i>25</i> |
| <i>Figure 10: Residual stresses measured at the surface of location 1 (i.e. radially into the corner of channel #2 from the specimen outer diameter surface) using ICHD and DHD.....</i> | <i>26</i> |
| <i>Figure 11: DHD measured residual stresses at location 1 (i.e. radially into the corner of channel #2 from the specimen outer diameter surface).</i> | <i>26</i> |
| <i>Figure 12: DHD measured residual stresses at location 2 (i.e. axially within the bulk material between channels #3 and #4, and the specimen outer diameter surface).</i> | <i>27</i> |
| <i>Figure 13: Residual stresses measured at the surface of location 3 (i.e. radially through the axis of the specimen from the outer diameter surface between channels #2 and #4) using ICHD and DHD.</i> | <i>28</i> |
| <i>Figure 14: DHD measured residual stresses at location 3 (i.e. radially through the axis of the specimen from the outer diameter surface between channels #2 and #4).....</i> | <i>28</i> |

1 INTRODUCTION

VEQTER Ltd was requested by SKB under purchase order 10225 to undertake a number of residual stress measurements in the nodular cast iron insert of a PWR radioactive waste canister. This report provides details of the measurements carried out under this order, more specifically, the measurement of bi-axial residual stresses using the Incremental Centre-Hole Drilling (ICHD) and Deep-Hole Drilling (DHD) techniques within the Cast Iron Insert provided by SKB.

2 SPECIMEN DESIGN

SKB supplied a short section of complete Nodular Cast Iron Insert IP25 to VEQTER Ltd's facilities in the UK. The complete Cast Iron Insert (\varnothing 960 mm \times 4595 mm long) was cast in the vertical position with the molten cast iron filling the voids in the mould between four steel tubes (260 mm \times 260 mm with a nominal wall thickness of 12.5 mm) set in a 2 \times 2 configuration, see Figure 1 and Figure 2. To maintain their relative positions and straightness during the casting process, the steel tubes were fixed at the bottom of the casting and to one another along their length using 100 mm wide steel plates welded between them every 800 mm.

The short section of Cast Iron Insert IP25 supplied measured 960 mm in diameter and roughly 750 mm in length, see Figure 2. The section had been cut from the original Cast Iron Insert from the region measuring 1455 - 2205 mm from the bottom of the steel tubes, see Figure 1. The 2205 mm end of the section had been identified by "2205" punched markings and the steel tubes were numbered 1 – 4 prior to arrival at VEQTER.

3 INCREMENTAL CENTRE-HOLE DRILLING PROCEDURE

The ICHD residual stress measurement technique is a semi-invasive, mechanical strain relief (MSR) technique (i.e. the strain of the component is measured during stress relief from the removal of a small amount of material) [1 - 4]. The ICHD procedure involves drilling a small hole into the surface of the component at the centre of a strain gauge rosette and measuring the relieved strains. The ICHD process consists of two main stages, i.e. 1) sample preparation involving the mounting of strain gauges and 2) the actual drilling process to relieve the strains to be recorded and measured.

Sample Preparation & Strain Gauging

Strain gauging is itself a three stage process involving surface preparation, gauge bonding and circuit connections. Surface preparation involved degreasing the surface at and around the measurement location with a chlorinated hydrocarbon solution to remove any oxides and oils. Surface irregularities were removed by light abrasion with silicon-carbide paper (grit designation-P400; average particle size-35.3 μ m) wet with mild phosphoric acid conditioner. The surface was then neutralised using an ammonia based solution. Two types of strain gauge rosette (i.e. types EA-06-031RE-120 and CEA-06-062UL-120), especially designed for ICHD measurements, were used depending on the measurement location, which will be discussed further later on in the report. Table 1 shows the type of strain gauge used along with its key dimensions. The strain gauges were adhered to the specimen with "M-Bond 200" with gauge elements in the hoop, axial and in-plane shear directions, see Figure 3. A quarter Wheatstone bridge circuit was formed by soldering the lead wires to the terminals of the gauge. A

Wheatstone bridge was used because of its inherent ability to detect small resistance changes produced in strain gauges, produce zero output voltage when the test part is unloaded and provide compensation for temperature induced resistance changes in the strain gauge circuit configuration [3]. The EA-06-031RE-120 gauges were purchased as 'pre-wired' to decrease the error in gauge calibration that can occur when manually applying lead wires to such small gauges.

Drilling Process

The computer-controlled, 3-axis, ICHD drilling machine was secured to the specimen during the drilling process with the drill axis aligned perpendicular to the strain gauge. The strain gauge lead wires were connected to a calibrated strain recording system which in turn was connected to a computer for data logging. A USB microscope was used to optically align the drill tip to the exact measurement location in the centre of the strain gauge. The establishment of zero depth was also performed optically, in real time, through the microscope focused on the drill tip and work surface as the drilling head was advanced towards the specimen. Zero depth was set at the point when the backing film of the strain gauge rosette was completely removed. The measurements were carried out by orbital drilling (i.e. the drill bit axis of rotation was offset from the centre of the strain gauge rosette and a "trepanning" motion was used to create the hole) using depth increments of 16 μm or multiples thereof to final depths of 1.12 mm and 1.408 mm for the small and large gauges respectively. Between each increment in depth drilled, the strains measured by all three elements of the strain gauge rosette were automatically recorded by the controlling computer.

Figure 4 shows a photograph of the ICHD drilling machine head aligned to the strain gauge rosette at location 1 immediately before drilling commences. Finally, the residual stresses were calculated from the recorded strains using the Integral Method [1, 2].

Technique Accuracy

During the ICHD process it is most likely that the strain gauge and strain indicator are the greatest sources of uncertainty in the form of noise in the strain output. The noise levels are significant within the first and last 20 % of the measured stress depths due to the low magnitudes of strain relaxation detected by the surface strain gauge and thus an increased noise to signal ratio. Also, there will be other uncertainties present within the calculated residual stresses due to the component (e.g. surface condition and preparation, geometry and material properties) and drilling factors (e.g. drill bit shape and condition, concentricity, depth control, and hole diameter). Other factors affecting the accuracy of the results lie in the fitting of the raw strain data and the influence coefficients used in the ICHD analysis. The errors presented in this report are those due to errors in diameter measurement, depth measurement, strain measurement and Young's Modulus, which are the easiest to define, relatively. Table 2 lists the main sources of uncertainty for this work and provides information on their effect on the calculated stress results according to [1 - 4].

4 DEEP-HOLE DRILLING PROCEDURE

The DHD residual stress measurement technique is also a semi-invasive, MSR technique. The procedure used for the DHD technique can be divided into 5 stages [5], as shown in Figure 5 for a simple welded component:

1. Reference bushes are attached to the front and back surfaces of the component at the measurement location.
2. A reference hole is gundrilled through the component and reference bushes.
3. The diameter, \varnothing_0 , of the reference hole is measured through the entire thickness of the component and reference bushes using an air-probe. Diameter measurements are taken at 0.2 mm increments in depth and at 22.5 ° increments in angle about the axis of the reference hole.
4. A cylinder (i.e. core) of material, containing the reference hole along its axis is cut from the component using electro-discharge machining (EDM).
5. The diameter, \varnothing , of the reference hole is re-measured through the entire thickness of the cylinder and reference bushes. Diameter measurements are taken at the same locations as those measured in Stage 3.

The diameter, \varnothing_0 , of the reference hole measured in Stage 3 is the diameter when stresses are present. During Stage 4 the stresses are relieved, hence the diameter, \varnothing , of the reference hole measured in Stage 5 is the diameter when stresses are not present. The differences between the measured diameters in Stages 3 and 5 enable the original residual stresses to be calculated.

Technique Accuracy

Because the technique measures diameters at Stage 3 (stressed state) and Stage 5 (unstressed state) a true stress profile can be generated without the need for material response coefficients as with most mechanical strain relaxation techniques. Therefore the measurement accuracy is independent of depth and specimen thickness.

Although the DHD technique is indifferent to the surface finish of the component, there are surface phenomena that affect the accuracy of shallow measurements, or measurements near a free surface. The bushes applied in Stage 1 of the DHD procedure help to minimise most of the experimental equipment errors that occur near the entrance and exit of the reference hole at the specimen surfaces, e.g. bell-mouthing of the reference hole and air-probe air flow effects. However elasticity surface effects also occur at these surfaces that alter the shape of the reference hole and due to the difficulty in incorporating these effects, which can only be accounted for using modelled coefficients, some DHD surface results have been omitted. All the results submitted in this report are accurate to the detailed uncertainty analysis of the DHD technique published by Goudar et al [6]. Goudar et al discussed different approaches leading to the evaluation of uncertainties, however for practical purposes, only the uncertainties based on the propagation of errors has been incorporated for this work. Therefore the errors presented here for the measurements undertaken comprise of:

1. Calibration Error – due to a combination of human and instrument error in the calibration of the air-probe before and after measuring the reference hole diameter.
2. Curve-fit Error – due to the curve fitting of the air-probe calibration data.

3. Misalignment Error – accounting for surface roughness of the reference hole and core extension.
4. Material Constant – Young’s modulus error – generally a 5 % uncertainty is assumed unless the data provided by the client informs us otherwise.

The above parameters contain the major sources of uncertainty in the measured residual stresses using the DHD technique. However, other sources of uncertainty, including; exclusion of the third strain component, effects of the 2θ ‘strain fit’ calculations and the analytical assumption of independent block lengths of material are difficult to characterise and therefore not included, but nevertheless they are thought to be relatively negligible. The uncertainty due to air-probe angular misalignment presented by Goudar et al [6] using random number analysis cannot be obtained via experiment and hence is also not included. However, based on the random number analysis, uncertainty due to angular misalignment is negligible compared to the other sources of uncertainty.

5 MEASUREMENT LOCATIONS

There were two ICHD and three DHD measurements made in total in the Nodular Cast Iron Insert specimen. Each measurement line was defined by SKB, as shown in Figure 6, and then carried out at a suitable distance from specimen mid-length so as not to be influenced by each other, the free-ends of the specimen or the 100 mm wide steel connecting plates.

ICHD1 + DHD1

ICHD1 and DHD1 were carried out at the same location at 356 mm from the “2205” end and drilling radially inwards to penetrate through the corner of steel tube channel 2, see Figure 6 and Figure 7. At this location the DHD process was carried out using a \varnothing 1.5 mm reference hole and extracting a \varnothing 5 mm core, therefore the ICHD process was carried out using SGR type EA-06-031RE-120 and drilling a hole of 1.12 mm diameter up to a depth of 1.1 mm. The smaller sized SGR was used at this location in order to keep the ICHD hole size below that of the DHD reference hole.

DHD2

DHD2 was carried out by drilling axially from the “2205” end in the middle of the material between steel tube channels 3 and 4, and the outer surface, see Figure 6 and Figure 8 for clarification. No ICHD measurement was carried out at this location. The DHD technique was carried out by drilling a \varnothing 3 mm reference hole completely through the specimen and trepanning a \varnothing 10 mm core up to a depth of 522 mm only, therefore the DHD core remains attached to the specimen. An EDM depth of 522 mm was deemed sufficient to relieve the residual stress acting on the reference hole up to the desired total measurement depth of 500 mm.

Due to the large depth of measurement the reference hole was gundrilled in three stages with changes in drill at 213 mm and 385 mm deep. Also, two separate air-probes were used to measure the diameter of the reference hole before and after EDM trepanning. A short air-probe was used to gain data from 0 mm – 330 mm deep and a longer air-probe was used to measure data from 255 mm – 560 mm deep. The overlap in measured data enabled the separate residual stresses calculated from each air-probe measurement to be spliced together at 280 mm depth.

ICHD3 + DHD3

ICHD3 and DHD3 were carried out at the same location at 305 mm from the “2205” end and drilling radially inwards between steel tube channels 2 and 4 to intersect with the axis of the specimen, see Figure 6 and Figure 9. At this location the DHD technique was carried out by drilling a $\varnothing 3$ mm reference hole completely through the specimen and trepanning a $\varnothing 10$ mm core up to a depth of 494 mm only, therefore the DHD core remains attached to the specimen. An EDM depth of 494 mm was deemed sufficient to relieve the residual stress acting on the reference hole up to the desired total measurement depth of 480 mm. With the larger $\varnothing 3$ mm reference hole, the ICHD process was carried out using SGR type CEA-06-062UL-120 and drilling a hole of 1.84 mm diameter up to a depth of 1.408 mm. The larger sized SGR was used at this location due to improved accuracies, but still keeping the ICHD hole size below that of the DHD reference hole.

Again, due to the large depth of measurement the reference hole was gundrilled in three stages with changes in drill at 250 mm and 428 mm deep. Also, two separate air-probes were used to measure the diameter of the reference hole before and after EDM trepanning. A short air-probe was used to gain data from 0 mm – 321 mm deep and a longer air-probe was used to measure data from 271 mm – 550 mm deep. The overlap in measured data enabled the separate residual stresses calculated from each air-probe measurement to be spliced together at 293 mm depth.

6 RESULTS AND DISCUSSION

The analyses used to convert the measured raw data into residual stresses for both the ICHD and DHD measurements assumed isotropic, plane stress conditions with a Young's Modulus, E , of 159.9 GPa and a Poisson's ratio of 0.32 for all measurement depths. The Poisson's ratio however was not required for the DHD analysis due to the assumed isotropic, plane stress conditions. All stresses have been tabulated and plotted as functions of depth below the surface of the specimen. For the ICHD1 + DHD1 and ICHD3 + DHD3 measurements with the hole drilled radially, the residual stresses measured were those acting in the hoop and axial directions along with their in-plane shear. Whereas for DHD2, drilled axially, the residual stresses measured were those acting in the hoop and radial directions along with their in-plane shear. The axes notation can be seen in Figure 7 to Figure 9. In this report only a reduced data set (i.e. not including all the calculated data points) is tabulated for the DHD results in order to reduce the size of the report, however the plotted results show the complete data set.

ICHD1 + DHD1

The residual stresses measured at this location using the ICHD and DHD techniques are recorded in Table 3 and Table 4, and shown in Figure 10 and Figure 11. The axial and hoop residual stresses were found to be similar in profile (i.e. uniform throughout), predominantly compressive and low in magnitude. At accurate depths for the ICHD technique (i.e. at depths greater than 20 % of total measurement depth) the hoop residual stresses were found to be the most tensile by an average of 9 MPa. Whereas for the DHD measurement the axial residual stresses were found to be the most tensile by an average of 17 MPa. Throughout the measurement depths the fluctuations of the axial and hoop stress profiles are below the accuracy of the DHD technique and as such are not described.

At ICHD depths above 0.1 mm (i.e. the 20 % depth accuracy band) the axial and hoop residual stresses were found to start at -47 MPa and -46 MPa, and increase passing through zero at 0.4 mm and 0.3 mm, to reach 15 MPa and 26 MPa at the final depth measured of 0.4875 mm, all respectively.

For the DHD results, the axial residual stresses gradually and proportionately increased from roughly -24 MPa at 0.6 mm depth to -9 MPa at 42.2 mm depth with average fluctuations of only 2.8 MPa. Whereas the hoop residual stresses remained approximately constant at -33 MPa with average fluctuations of only 3.2 MPa. The shear stresses were found to be negligible throughout with an average value of 1.8 MPa and a standard deviation of 2.7 MPa.

The axial and hoop mean error values for this measurement were both ± 16 MPa with standard deviations of 1.2 MPa and 1.6 MPa respectively.

DHD2

The residual stresses measured at this location using just the DHD technique are recorded as a reduced data set in Table 5 with the complete data set shown in Figure 12. The radial and hoop stresses were found to be equi-biaxial up to 390 mm depth after which the radial residual stresses become more compressive. The radial and hoop residual stresses start in compression at the cut surface at -15 MPa and -7 MPa respectively, before temporarily increasing into tension to reach 11 MPa and 30 MPa, respectively, at roughly 5 mm depth and then back into compression reaching -29 MPa and -25 MPa, respectively, at 9.2 mm depth. The radial and hoop residual stresses then gradually increased to reach -14 MPa and -10 MPa, respectively, at 128.8 mm at which depth they rapidly decreased to -35 MPa at 148.4 mm. The radial and hoop residual stresses then increased turning into tension at roughly 262 mm to reach 10 MPa at 275 mm at which they both remained until roughly 360 mm depth. The hoop residual stresses remained at roughly 10 MPa until the final depth measured at 550 mm, whereas the radial residual stresses decreased back into compression to roughly -14 MPa at 422 mm before gradually increasing to 4 MPa at the final depth measured, i.e. 550 mm.

The shear residual stresses peaked in tension at 23 MPa within the first 5 mm depth, then rapidly decreased to fluctuate between -20 MPa and -5 MPa from 6 mm to 150 mm, after which they remained at a mean of -8 MPa from 150 mm to 550 mm with an associated standard deviation of 5 MPa.

The radial and hoop mean error values for this measurement were both ± 11 MPa with standard deviations of 2.5 MPa and 2.6 MPa respectively.

ICHD3 + DHD3

The residual stresses measured at this location using the ICHD and DHD techniques are recorded in Table 6 and Table 7, and shown in Figure 13 and Figure 14. The axial and hoop residual stresses were found to be similar in profile, low in magnitude and predominantly compressive except in the two regions adjacent to the wall of the steel tubes running at 90 ° to the measurement axis, see Figure 6 for identification of these regions in blue.

At ICHD depths above 0.2 mm (i.e. the 20 % depth accuracy band) the axial and hoop residual stresses were found to be predominantly compressive with the hoop residual stresses being

the most tensile by roughly 50 MPa at depths up to 0.625 mm and then becoming equi-biaxial. The axial and hoop residual stresses were found to start at -179 MPa and -119 MPa respectively, and increase passing through zero at roughly 0.9 mm to reach 21 MPa and 12 MPa, respectively, at the final depth measured of 0.975 mm.

The initial DHD results agree very well with the final ICHD results, showing roughly zero stress magnitudes with the axial stresses being the most tensile. The axial residual stresses were predominantly compressive throughout, maintaining an average magnitude of -8 MPa with an associated standard deviation of 4 MPa, apart from the regions adjacent to the steel tube walls running at 90 °, as previously defined. Whereas the hoop residual stresses started at -5 MPa, decreased to -22 MPa at 8.8 mm before increasing to 0 MPa at 112 mm. At greater depths the hoop residual stresses remained approximately constant with a mean value of 1 MPa and associated standard deviation of 4 MPa, apart from the regions adjacent to the steel tube walls running at 90 °, again. For the regions adjacent to the steel tube walls running at 90 °, the axial and hoop residual stresses reach tensile peaks from 40 MPa to 90 MPa with the hoop residual stresses being the most tensile, as could be expected, by roughly 20 MPa. For these regions, the residual stresses increase rapidly to reach and maintain constant peak values for roughly 23 mm and then decrease rapidly again to the nominally low stress magnitudes. The peak magnitudes at the outer most region (i.e. 156 mm – 180 mm depth) was measured to be roughly 10 MPa higher than the inner region (i.e. 400 mm – 421 mm depth).

The shear stresses were found to be negligible throughout with an average value of -2.3 MPa and a standard deviation of 2.3 MPa.

The noise levels within the results can be seen to change at 292.8 mm which is the depth at which the results change from being measured using the short or long air-probe. However the noise levels are well within the errors calculated for the results at ± 12 MPa with standard deviations of 1.6 MPa and 1.8 MPa for the axial and hoop residual stresses respectively.

General DHD Comments

From previous calibration studies, the nominal, empirical accuracy of the DHD residual stress measurement technique will be ± 24 MPa [7] assuming isotropic material properties and a Young's modulus of 159.9 GPa. However, this general accuracy cannot be applied to the measured residual stresses at depths within 0.5 mm of a free surface. At these depths surface edge effects occur and the accuracy of the air gauging equipment and hence measured residual stresses are unknown. Therefore, the measured residual stresses over these depths have been omitted from the tabular and graphical results to avoid confusion.

Bonner [8] studied the effect of stress gradients acting across a $\varnothing 20$ mm core and the resulting distortions of a coaxial $\varnothing 3.2$ mm reference hole. Bonner found that the measured distortions of the reference hole were due to the relaxation of residual stresses across the entire cross-sectional area of the extracted core. However, Bonner also found that the distortions of the reference hole were approximately eight times more sensitive to the stresses acting at the centre-line of the reference hole than to those acting near the outer diameter of the core.

7 CONCLUSIONS

A 750 mm long section of a PWR Nodular Cast Iron Insert containing four steel tubes was supplied by SKB for measurement. Bi-axial residual stress profiles were measured using the ICHD and DHD techniques along three measurement lines prescribed by SKB.

Measurement lines 1 and 3 were radially inwards from the specimen outer surface using the ICHD and DHD techniques, and measuring the hoop and axial residual stresses. Measurement line 2 was carried out axially using just the DHD technique, providing the hoop and radial residual stresses.

For the measurement into the steel tube at its closest proximity to the outer surface of the Insert (i.e. measurement location 1) the axial and hoop residual stresses were found to be compressive and approximately constant at roughly -24 MPa and -35 MPa respectively.

For the measurement running axially through the bulk material zone at 70 mm from the Insert outer surface (i.e. measurement location 2), the radial and hoop residual stresses were found to be predominantly equi-biaxial, varying between -30 MPa and 20 MPa.

For the measurement carried out radially into the centre of the Insert between two steel tubes (i.e. measurement location 3) the axial and hoop residual stresses were low in magnitude within ± 10 MPa, apart from the two regions adjacent to the steel tube walls running at 90 °. Within these regions the axial and hoop residual stresses reach tensile peaks from 40 MPa to 90 MPa with the hoop residual stresses being the most tensile, as could be expected, by roughly 20 MPa.

Compressive residual stresses were found at the surface of the Cast Iron Insert specimen using the ICHD technique.

An overall nominal accuracy of approximately ± 24 MPa is valid for the DHD residual stress measurements at all depths, except at those within 0.5 mm of the specimen surface. Based on this error band, many of the 'features' in the residual stress profiles could be considered to be measurement fluctuations and were not necessarily due to a changing stress field, but more likely a result of the errors and inaccuracies of the measurement technique.

8 REFERENCES

- [1]. **Schajer G.S.**, "*Measurement of Non-Uniform Residual Stresses Using the Hole Drilling Method*", Journal of Engineering Material Technology, 1988, Vol. 110, No. 4, Part1: pp. 338-343, Part 2: pp. 344-349.
- [2]. **ASTM-E837-08**, "*Standard Test Method for Determining Residual Stresses by the Hole-drilling Technique*", ASTM International, 2008.
- [3]. **Vishay Precision Group**, "*Measurement of Residual Stresses by the Hole-Drilling Strain Gage Method*", <http://www.vishaypg.com/docs/11053/tn503.pdf>, Document Number: 11053, [Online] 01 November 2010.

[4]. **Grant, P.V. et al.**, “*The Measurement of Residual Stresses by the Incremental Hole Drilling Technique*”, Measurement Good Practice Guide No. 53, NPL, UK, 2002.

[5]. **Kingston, E.J. et al.**, “*Novel Applications of the Deep-Hole Drilling Technique for Measuring Through-Thickness Residual Stress Distributions*”, Journal of ASTM International, April 2006, Vol. 3, No. 4.

[6]. **Goudar, D.M. et al.**, “*Evaluating Uncertainty in residual stress measured using the deep-hole drilling technique*”, Strain, 2009, Vol. 47, pp: 62-74.

[7]. **George, D.F.B. et al.**, “*Measurement of Through-Thickness Stresses Using Small Holes*”, Journal of Strain Analysis for Engineering Design, 2002, No. 2, Vol. 7.

[8]. **Bonner, N.W.**, “*Measurement of Residual Stress in Thick-Section Steel Welds*”, University of Bristol, PhD Thesis, 1996.

9 TABLES

Table 1: A table listing the important dimensions of the EA-06-031RE-120 and CEA-06-062UL-120 strain gauges used for ICHD measurements (Dimensions in blue in mm) [6].


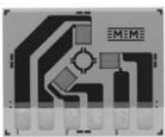
| GAGE PATTERN AND DESIGNATION Insert Desired S-T-C No. in Spaces Marked XX. See Note 1 | | RES. IN OHMS | DIMENSIONS | | | | | |
|--|---|--------------------------|--|--------------------------|-------------------|------|--------|-------|
| | | | GAGE LENGTH | GRID CTR'LINE DIA. | TYPICAL HOLE DIA. | | MATRIX | |
| | | | | | Min. | Max | Length | Width |
| EA-XX-031RE-120 EA-XX-031RE-120/SE |  | 120 ± 0.2% 120 ± 0.4% | 0.031 | 0.101 | 0.03 | 0.04 | 0.29 | 0.29 |
| | | | 0.79 | 2.56 | 0.8 | 1.0 | 7.4 | 7.04 |
| | | | Due to small pattern size, measurement error can be magnified by slight mislocation of drill hole. Pattern not recommended for general-purpose applications. | | | | | |
| CEA-XX-062UL-120 |  | 120 ± 0.4% | 0.062 | 0.202 | 0.06 | 0.08 | 0.50 | 0.62 |
| | | | 1.57 | 5.13 | 1.5 | 2.0 | 12.7 | 15.7 |
| | | | Fully encapsulated with large copper-coated soldering tabs. Same pattern geometry as 062RE pattern. | | | | | |

Table 2: Sources of uncertainty in the ICHD technique and their influence on this work.

| Source of Uncertainty | Uncertainty / Contribution | Application specific comments |
|---|---------------------------------------|--|
| Component | | |
| Geometry | Negligible | Large component. |
| Level of stresses present | Negligible | Low stress component so no chance of plastic stress relaxation. |
| Out-of-plane stress gradients | Negligible | Low stress component. |
| Poisson's Ratio | Negligible | Low stress component. |
| Surface condition (e.g. texture, roughness, flatness) | Negligible | Component already supplied with good surface condition. Large component. |
| Young's Modulus | Included in the uncertainty analysis. | |

| | | |
|---|--------------------------------------|---|
| Measurement system | | |
| Quality of drilling equipment | Negligible | Equipment validated by checking measurements of known stress fields, e.g. plastically bent beam. |
| Quality of strain gauges (dimensions, temperature compensation, geometry) | Negligible | Use of controlled supplier. Strain gauges connected to compensate for temperature changes. |
| Quality of strain measurement equipment | Negligible | Calibrated equipment from controlled supplier. |
| Measurement procedure | | |
| Concentricity of hole to strain gauge rosette | Negligible | If out of tolerance then a new measurement is carried out. |
| Definition of zero depth | Negligible | Zero depth detected using optical microscope whilst drilling incrementally advanced. |
| Drilled hole shape | Negligible | Computer controlled machining with a new drill used for each measurement. |
| Drilling depth precision | Included in the uncertainty analysis | |
| Drilling induced stresses and temperature changes | Negligible | Temperature compensating strain gauges used. High-speed, orbital drilling used. New drill used for each measurement. Constant coolant air flow used during whole measurement. |
| Measurement of drilled hole diameter | Included in the uncertainty analysis | |
| Perpendicularity of hole axis to strain gauge surface | Negligible | Large Component. Contribution depends on hole depth. |
| Proximity of measurement locations | Negligible | Spacing is >10 times the drilled hole diameter |
| Quality of strain gauge installation (surface preparation, bonding, wiring) | Minimised | Personnel trained and certified by external body. |
| Strain gauge errors (drift, non-zeroing) | Negligible | Zero readings immediately before measurement start. Short measuring cycle. |
| Strain measurement | Included in the uncertainty analysis | |
| Operator | | |
| Operator skill | Minimised | Personnel trained and certified in-house. High frequency of measurements carried out so high skill level maintained. |
| Environment | | |
| Temperature changes and humidity | Negligible | Lab-based measurements away from inclement conditions |
| Analysis | | |
| Raw data smoothing/fitting | Negligible at depths >10 % - 20 % | |
| Data analysis method | Minimised | Non-uniform stress analysis, i.e. the Integral Method |

Table 3: ICHD residual stress measurement results at location 1.

| Depth (mm) | Axial Stress (MPa) | Hoop Stress (MPa) | Shear Stress (MPa) | Axial Error (MPa) | Hoop Error (MPa) | Shear Error (MPa) |
|------------|--------------------|-------------------|--------------------|-------------------|------------------|-------------------|
| 0.0125 | 121.4 | -50.2 | 221.5 | 12.5 | 8.9 | 43.0 |
| 0.0375 | 10.8 | -69.9 | 38.3 | 14.7 | 13.7 | 56.0 |
| 0.0625 | -41.0 | -71.6 | 19.5 | 13.6 | 11.3 | 52.6 |
| 0.0875 | -50.6 | -59.7 | 45.3 | 14.4 | 11.7 | 51.4 |
| 0.1125 | -47.0 | -46.2 | 55.9 | 14.2 | 10.6 | 48.9 |
| 0.1375 | -41.8 | -36.6 | 56.2 | 14.5 | 11.9 | 50.6 |
| 0.1625 | -37.0 | -30.2 | 52.8 | 14.4 | 12.7 | 47.1 |
| 0.1875 | -32.6 | -24.6 | 45.5 | 16.4 | 13.4 | 50.7 |
| 0.2125 | -27.3 | -19.5 | 38.3 | 17.2 | 14.2 | 51.0 |
| 0.2375 | -21.9 | -14.5 | 30.2 | 17.8 | 14.6 | 62.1 |
| 0.2625 | -16.8 | -9.3 | 21.1 | 19.5 | 16.3 | 61.2 |
| 0.2875 | -12.1 | -4.5 | 12.1 | 23.8 | 19.0 | 56.7 |
| 0.3125 | -8.4 | -0.4 | 3.1 | 24.3 | 20.6 | 72.7 |
| 0.3375 | -5.6 | 3.2 | -6.0 | 28.6 | 24.2 | 74.2 |
| 0.3625 | -3.3 | 6.5 | -14.0 | 34.6 | 31.0 | 79.9 |
| 0.3875 | -1.2 | 10.0 | -21.1 | 40.3 | 33.7 | 83.8 |
| 0.4125 | 1.3 | 13.8 | -26.5 | 43.2 | 39.1 | 74.1 |
| 0.4375 | 4.8 | 17.6 | -29.6 | 55.7 | 51.8 | 94.2 |
| 0.4625 | 9.4 | 21.6 | -30.3 | 66.9 | 62.3 | 104.7 |
| 0.4875 | 14.5 | 25.5 | -29.6 | 82.2 | 72.9 | 112.8 |

Table 4: DHD residual stress measurement results at location 1.

| Depth (mm) | Axial Stress (MPa) | Hoop Stress (MPa) | Shear Stress (MPa) | Axial Error (MPa) | Hoop Error (MPa) | Shear Error (MPa) |
|------------|--------------------|-------------------|--------------------|-------------------|------------------|-------------------|
| 0.0-0.8 | Omitted | | | | | |
| 1.0 | -24.0 | -29.9 | 3.1 | 23.2 | 17.4 | 9.6 |
| 2.0 | -9.7 | -23.4 | 5.9 | 16.2 | 16.1 | 9.2 |
| 3.0 | -17.3 | -28.4 | 5.5 | 16.3 | 16.5 | 9.3 |
| 4.0 | -23.1 | -33.8 | 4.9 | 16.2 | 16.2 | 9.2 |
| 5.0 | -25.0 | -36.2 | 4.5 | 16.3 | 16.2 | 9.3 |
| 6.0 | -28.1 | -35.0 | 4.3 | 16.2 | 16.2 | 9.3 |
| 7.0 | -24.2 | -29.3 | 4.8 | 16.3 | 16.2 | 9.3 |
| 8.0 | -21.7 | -36.5 | 5.9 | 16.2 | 16.2 | 9.2 |
| 9.0 | -25.0 | -38.5 | 2.9 | 16.3 | 16.3 | 9.3 |
| 10.0 | -18.8 | -38.0 | 3.5 | 16.2 | 16.1 | 9.3 |
| 11.0 | -19.3 | -37.3 | 2.1 | 16.1 | 16.3 | 9.3 |
| 12.0 | -19.6 | -38.2 | 0.7 | 16.2 | 16.2 | 9.3 |
| 13.0 | -21.9 | -34.8 | 2.9 | 16.1 | 16.3 | 9.3 |
| 14.0 | -23.5 | -33.7 | -1.6 | 16.6 | 17.0 | 9.3 |

| Depth (mm) | Axial Stress (MPa) | Hoop Stress (MPa) | Shear Stress (MPa) | Axial Error (MPa) | Hoop Error (MPa) | Shear Error (MPa) |
|------------|--------------------|-------------------|--------------------|-------------------|------------------|-------------------|
| 15.0 | -23.8 | -36.5 | -2.1 | 16.5 | 16.7 | 9.3 |
| 16.0 | -23.5 | -38.8 | 0.7 | 16.1 | 16.1 | 9.4 |
| 17.0 | -17.4 | -33.4 | 0.6 | 16.1 | 16.2 | 9.3 |
| 18.0 | -19.9 | -28.4 | -0.2 | 16.2 | 16.1 | 9.2 |
| 19.0 | -20.7 | -34.9 | 1.4 | 16.2 | 16.2 | 9.3 |
| 20.0 | -16.0 | -36.1 | 1.6 | 16.2 | 16.1 | 9.3 |
| 21.0 | -15.5 | -37.6 | 4.3 | 16.2 | 16.3 | 9.3 |
| 22.0 | -15.2 | -33.7 | 2.3 | 16.5 | 16.2 | 9.4 |
| 23.0 | -18.9 | -31.5 | 3.7 | 16.2 | 16.1 | 9.3 |
| 24.0 | -16.1 | -31.7 | 0.8 | 16.1 | 16.2 | 9.3 |
| 25.0 | -16.0 | -31.8 | -0.5 | 17.1 | 16.4 | 9.4 |
| 26.0 | -15.2 | -35.0 | -1.0 | 16.3 | 16.3 | 9.5 |
| 27.0 | -12.9 | -38.7 | 1.0 | 16.1 | 16.3 | 9.4 |
| 28.0 | -7.9 | -31.6 | 1.8 | 16.4 | 16.1 | 9.4 |
| 29.0 | -10.4 | -24.9 | 1.0 | 16.6 | 16.5 | 9.4 |
| 30.0 | -18.0 | -33.9 | 0.8 | 16.2 | 16.1 | 9.3 |
| 31.0 | -13.4 | -35.6 | 2.1 | 16.4 | 16.4 | 9.4 |
| 32.0 | -12.4 | -33.0 | 3.2 | 16.4 | 16.3 | 9.3 |
| 33.0 | -8.0 | -35.6 | 6.2 | 16.4 | 16.3 | 9.3 |
| 34.0 | -10.7 | -34.6 | 3.2 | 16.2 | 16.3 | 9.3 |
| 35.0 | -10.1 | -34.0 | 1.4 | 16.3 | 16.4 | 9.4 |
| 36.0 | -12.7 | -34.5 | 1.4 | 16.1 | 16.2 | 9.3 |
| 37.0 | -10.0 | -34.9 | -0.2 | 16.0 | 16.2 | 9.4 |
| 38.0 | -12.1 | -37.6 | -3.6 | 16.0 | 16.5 | 9.3 |
| 39.0 | -9.9 | -34.0 | -2.8 | 17.4 | 16.6 | 9.4 |
| 40.0 | -15.4 | -27.7 | -3.7 | 16.6 | 17.6 | 9.3 |
| 41.0 | -4.8 | -20.1 | -2.0 | 16.1 | 16.2 | 9.3 |
| 42.0 | -4.5 | -25.2 | 0.2 | 16.2 | 16.4 | 9.4 |

Table 5: DHD residual stress measurement results at location 2.

| Depth (mm) | Radial Stress (MPa) | Hoop Stress (MPa) | Shear Stress (MPa) | Radial Error (MPa) | Hoop Error (MPa) | Shear Error (MPa) |
|------------|---------------------|-------------------|--------------------|--------------------|------------------|-------------------|
| 10 | -26.6 | -22.5 | -15.4 | 9.1 | 9.1 | 5.2 |
| 20 | -25.0 | -16.8 | -17.9 | 9.2 | 9.1 | 5.4 |
| 30 | -13.6 | -11.2 | -17.1 | 12.8 | 13.0 | 5.8 |
| 40 | -13.0 | -11.9 | -17.0 | 11.6 | 13.2 | 5.2 |
| 50 | -20.6 | -22.7 | -16.0 | 9.2 | 9.3 | 5.4 |
| 60 | -23.2 | -16.9 | -19.6 | 9.3 | 9.4 | 5.2 |
| 70 | -21.0 | -22.8 | -18.4 | 9.1 | 9.2 | 5.3 |
| 80 | -22.7 | -16.3 | -9.5 | 9.3 | 9.3 | 5.3 |
| 90 | -18.6 | -15.5 | -12.1 | 9.9 | 9.3 | 5.2 |

| Depth (mm) | Radial Stress (MPa) | Hoop Stress (MPa) | Shear Stress (MPa) | Radial Error (MPa) | Hoop Error (MPa) | Shear Error (MPa) |
|---------------|---------------------------|-------------------------|--------------------------|--------------------------|------------------------|-------------------------|
| 100 | -15.1 | -12.8 | -13.1 | 9.1 | 9.1 | 5.2 |
| 110 | -17.6 | -12.5 | -13.0 | 9.6 | 9.5 | 5.2 |
| 120 | -15.3 | -14.7 | -13.3 | 9.1 | 9.2 | 5.3 |
| 130 | -20.8 | -19.2 | -11.3 | 9.1 | 9.1 | 5.2 |
| 140 | -29.0 | -19.9 | -9.4 | 9.1 | 9.1 | 5.3 |
| 150 | -30.9 | -27.8 | -3.7 | 9.2 | 9.7 | 5.2 |
| 160 | -35.3 | -32.8 | -6.6 | 9.3 | 9.5 | 5.2 |
| 170 | -31.1 | -27.4 | -7.0 | 9.1 | 9.5 | 5.2 |
| 180 | -29.4 | -29.7 | -4.0 | 9.5 | 9.5 | 5.2 |
| 190 | -22.0 | -20.2 | -4.1 | 9.1 | 9.2 | 5.2 |
| 200 | -17.6 | -18.8 | -6.0 | 9.0 | 9.1 | 5.3 |
| 210 | -13.9 | -16.0 | -1.1 | 9.1 | 9.1 | 5.3 |
| 220 | -7.9 | -5.9 | -4.6 | 12.1 | 11.3 | 5.3 |
| 230 | -15.9 | -7.0 | -4.6 | 9.2 | 9.5 | 5.7 |
| 240 | -11.5 | -6.3 | -2.6 | 9.5 | 9.5 | 5.2 |
| 250 | -8.4 | -5.8 | -4.1 | 11.1 | 11.8 | 5.2 |
| 260 | -3.6 | -8.3 | -5.0 | 9.3 | 9.2 | 5.9 |
| 270 | 1.6 | -3.0 | -8.2 | 9.4 | 9.0 | 5.2 |
| 280 | 5.8 | 10.8 | -8.2 | 9.3 | 9.2 | 5.3 |
| 290 | 2.1 | 10.8 | -2.0 | 11.7 | 12.1 | 7.3 |
| 300 | 8.7 | 15.0 | -0.7 | 11.8 | 12.1 | 6.7 |
| 310 | 10.4 | 15.3 | -3.3 | 12.0 | 11.8 | 6.7 |
| 320 | 6.7 | 15.0 | -3.6 | 11.7 | 11.9 | 6.7 |
| 330 | 0.1 | 11.9 | -3.0 | 12.5 | 11.9 | 6.8 |
| 340 | 7.3 | 8.0 | -4.8 | 12.1 | 12.3 | 6.8 |
| 350 | 10.0 | 11.7 | -2.4 | 11.9 | 11.9 | 6.8 |
| 360 | 8.2 | 7.7 | -2.1 | 12.1 | 12.2 | 6.8 |
| 370 | 4.2 | 11.3 | -4.1 | 11.8 | 12.0 | 6.9 |
| 380 | 9.9 | 7.2 | -6.6 | 12.3 | 12.1 | 6.9 |
| 390 | 2.0 | 6.4 | -5.4 | 11.7 | 11.7 | 6.8 |
| 400 | 4.0 | 9.8 | -6.0 | 11.9 | 11.9 | 6.8 |
| 410 | -7.1 | 6.1 | -1.0 | 13.1 | 14.6 | 6.8 |
| 420 | -6.6 | 9.8 | -5.2 | 11.9 | 11.9 | 6.7 |
| 430 | -9.5 | 7.1 | -13.3 | 13.9 | 15.4 | 6.7 |
| 440 | -10.9 | 7.6 | -6.7 | 11.9 | 11.7 | 6.8 |
| 450 | 8.5 | 13.4 | -7.8 | 17.8 | 19.1 | 6.9 |
| 460 | -4.5 | 6.6 | -9.8 | 11.6 | 11.8 | 6.8 |
| 470 | -6.7 | 14.0 | -8.7 | 13.0 | 11.9 | 6.7 |
| 480 | -7.6 | 5.3 | -8.2 | 11.6 | 12.2 | 6.8 |
| 490 | -5.0 | 12.5 | -6.0 | 11.7 | 11.6 | 6.7 |
| 500 | -8.3 | 12.6 | -7.5 | 12.9 | 12.4 | 6.7 |
| 510 | -3.5 | 9.5 | -6.1 | 11.6 | 11.8 | 6.8 |
| 520 | -2.8 | 14.0 | -9.0 | 11.8 | 12.2 | 7.7 |

| Depth (mm) | Radial Stress (MPa) | Hoop Stress (MPa) | Shear Stress (MPa) | Radial Error (MPa) | Hoop Error (MPa) | Shear Error (MPa) |
|------------|---------------------|-------------------|--------------------|--------------------|------------------|-------------------|
| 530 | 0.0 | 13.6 | -1.5 | 13.0 | 11.8 | 7.9 |
| 540 | -10.3 | 21.5 | -3.8 | 11.6 | 12.4 | 7.9 |
| 550 | -0.6 | 17.0 | -2.1 | 14.4 | 13.3 | 6.8 |

Table 6: ICHD residual stress measurement results at location 3.

| Depth (mm) | Axial Stress (MPa) | Hoop Stress (MPa) | Shear Stress (MPa) | Axial Error (MPa) | Hoop Error (MPa) | Shear Error (MPa) |
|------------|--------------------|-------------------|--------------------|-------------------|------------------|-------------------|
| 0.025 | -175.7 | -163.0 | 15.3 | 12.1 | 11.8 | 11.3 |
| 0.075 | -192.8 | -153.3 | -3.4 | 18.0 | 16.8 | 16.9 |
| 0.125 | -198.4 | -141.2 | -21.0 | 17.0 | 16.1 | 16.1 |
| 0.175 | -191.2 | -129.1 | -31.8 | 17.4 | 15.5 | 15.1 |
| 0.225 | -178.7 | -118.9 | -34.7 | 15.5 | 14.6 | 13.3 |
| 0.275 | -167.0 | -111.1 | -32.1 | 18.0 | 15.1 | 14.9 |
| 0.325 | -157.5 | -105.3 | -26.3 | 18.4 | 17.0 | 15.2 |
| 0.375 | -148.7 | -100.4 | -19.3 | 19.4 | 18.2 | 16.5 |
| 0.425 | -138.9 | -95.6 | -12.3 | 20.6 | 19.5 | 16.7 |
| 0.475 | -127.2 | -90.2 | -6.3 | 21.8 | 21.4 | 16.3 |
| 0.525 | -112.3 | -83.2 | -2.2 | 24.4 | 21.6 | 16.5 |
| 0.575 | -95.5 | -75.6 | -0.1 | 27.6 | 26.5 | 19.5 |
| 0.625 | -77.9 | -68.2 | 0.2 | 28.5 | 28.5 | 21.6 |
| 0.675 | -60.1 | -61.2 | -0.8 | 31.0 | 29.6 | 20.8 |
| 0.725 | -42.8 | -53.6 | -2.4 | 40.6 | 40.8 | 25.7 |
| 0.775 | -26.6 | -44.5 | -3.6 | 50.4 | 46.4 | 28.3 |
| 0.825 | -12.1 | -33.4 | -3.4 | 51.3 | 50.2 | 27.0 |
| 0.875 | 0.3 | -19.9 | -1.2 | 58.9 | 56.9 | 33.3 |
| 0.925 | 11.2 | -4.3 | 2.8 | 78.6 | 74.2 | 36.4 |
| 0.975 | 21.2 | 12.2 | 7.7 | 109.5 | 106.7 | 34.8 |

Table 7: DHD residual stress measurement results at location 3.

| Depth (mm) | Axial Stress (MPa) | Hoop Stress (MPa) | Shear Stress (MPa) | Axial Error (MPa) | Hoop Error (MPa) | Shear Error (MPa) |
|------------|--------------------|-------------------|--------------------|-------------------|------------------|-------------------|
| 10 | -9.4 | -18.4 | -0.9 | 10.4 | 10.4 | 5.9 |
| 20 | -8.7 | -15.8 | -0.5 | 10.4 | 10.4 | 5.9 |
| 30 | -9.6 | -13.0 | -1.7 | 10.9 | 10.7 | 6.0 |
| 40 | -10.5 | -13.0 | 0.3 | 10.4 | 10.4 | 5.9 |
| 50 | -5.1 | -9.1 | -0.3 | 10.4 | 10.4 | 5.9 |
| 60 | -6.3 | -6.9 | -0.5 | 10.4 | 10.4 | 5.9 |
| 70 | -5.6 | -8.3 | -0.8 | 10.4 | 10.5 | 5.9 |

| Depth (mm) | Axial Stress (MPa) | Hoop Stress (MPa) | Shear Stress (MPa) | Axial Error (MPa) | Hoop Error (MPa) | Shear Error (MPa) |
|---------------|--------------------------|-------------------------|--------------------------|-------------------------|------------------------|-------------------------|
| 80 | -5.3 | -5.0 | -1.4 | 10.4 | 10.4 | 6.0 |
| 90 | -2.3 | -3.2 | -1.4 | 10.4 | 10.4 | 5.9 |
| 100 | -3.2 | -2.7 | -1.9 | 10.4 | 10.4 | 6.0 |
| 110 | -4.6 | -0.5 | -2.1 | 10.4 | 10.4 | 6.0 |
| 120 | -3.7 | 2.7 | -1.4 | 10.4 | 10.8 | 6.0 |
| 130 | -1.5 | 4.2 | -1.2 | 10.4 | 10.5 | 6.0 |
| 140 | -7.1 | 6.0 | 1.4 | 11.0 | 11.3 | 6.0 |
| 150 | -12.4 | 2.1 | -1.8 | 10.4 | 10.4 | 6.0 |
| 156 | -14.9 | 2.7 | -2.2 | 10.4 | 10.4 | 6.0 |
| 158 | -9.3 | 14.8 | -1.1 | 10.5 | 11.0 | 6.0 |
| 160 | -1.9 | 23.5 | 0.2 | 13.5 | 13.7 | 6.5 |
| 162 | 38.1 | 61.8 | -2.3 | 12.3 | 11.0 | 6.2 |
| 164 | 59.6 | 79.9 | -2.3 | 10.7 | 10.7 | 6.0 |
| 166 | 61.0 | 80.8 | -3.3 | 12.0 | 11.9 | 6.3 |
| 168 | 60.8 | 79.0 | -1.6 | 11.0 | 11.0 | 6.0 |
| 170 | 58.9 | 82.5 | -1.5 | 10.5 | 10.6 | 6.0 |
| 172 | 60.5 | 84.2 | -5.3 | 11.6 | 11.9 | 6.1 |
| 174 | 51.5 | 74.2 | -2.5 | 10.7 | 10.9 | 6.2 |
| 176 | 28.7 | 51.4 | -1.8 | 13.7 | 13.2 | 6.2 |
| 178 | -2.3 | 17.6 | -3.2 | 10.5 | 10.6 | 6.0 |
| 180 | -9.7 | 7.1 | -5.1 | 11.0 | 10.6 | 6.1 |
| 190 | -10.1 | 5.6 | -2.9 | 10.4 | 10.4 | 5.9 |
| 200 | -11.1 | -0.2 | -2.6 | 10.3 | 10.4 | 6.0 |
| 210 | -11.5 | 1.3 | -3.7 | 10.4 | 10.4 | 5.9 |
| 220 | -13.9 | -0.8 | -3.5 | 10.4 | 10.4 | 6.0 |
| 230 | -10.2 | 0.5 | -4.6 | 10.4 | 10.4 | 6.1 |
| 240 | -9.0 | -2.2 | -3.9 | 10.4 | 10.8 | 6.1 |
| 250 | -16.8 | -2.9 | -7.0 | 10.5 | 10.4 | 6.1 |
| 260 | -14.2 | 2.6 | -4.2 | 11.3 | 11.6 | 6.0 |
| 270 | -11.3 | -1.9 | -4.3 | 10.4 | 10.4 | 6.1 |
| 280 | -8.8 | -3.2 | -5.3 | 11.3 | 10.4 | 6.2 |
| 290 | -7.7 | -3.4 | -5.8 | 11.8 | 10.5 | 5.9 |
| 300 | -7.8 | -2.1 | -2.4 | 12.0 | 12.6 | 6.8 |
| 310 | 2.4 | 0.2 | 2.1 | 12.4 | 11.9 | 7.0 |
| 320 | 7.8 | 7.9 | 2.4 | 13.6 | 13.6 | 7.1 |
| 330 | 1.2 | -0.6 | 0.6 | 13.0 | 12.0 | 7.3 |
| 340 | -10.1 | -5.3 | -2.7 | 11.7 | 11.7 | 6.8 |
| 350 | -7.9 | -5.7 | -0.8 | 12.3 | 12.0 | 6.8 |
| 360 | -5.6 | -2.7 | -1.3 | 11.9 | 12.1 | 6.9 |
| 370 | 5.0 | 2.0 | 2.4 | 12.2 | 12.7 | 6.9 |
| 380 | -3.0 | 1.0 | 1.7 | 12.1 | 12.0 | 7.0 |
| 390 | -10.5 | 3.5 | -2.2 | 12.9 | 12.8 | 6.8 |
| 400 | -7.8 | 11.6 | -2.8 | 12.2 | 13.0 | 6.8 |

| Depth (mm) | Axial Stress (MPa) | Hoop Stress (MPa) | Shear Stress (MPa) | Axial Error (MPa) | Hoop Error (MPa) | Shear Error (MPa) |
|---------------|--------------------------|-------------------------|--------------------------|-------------------------|------------------------|-------------------------|
| 402 | 9.2 | 18.9 | 0.5 | 12.5 | 12.6 | 6.9 |
| 404 | 39.1 | 58.1 | -5.3 | 19.8 | 22.5 | 7.3 |
| 406 | 61.9 | 76.2 | 0.3 | 15.2 | 17.1 | 6.9 |
| 408 | 52.4 | 64.6 | -1.2 | 14.6 | 16.6 | 7.0 |
| 410 | 45.5 | 65.1 | -0.9 | 13.0 | 16.3 | 7.2 |
| 412 | 39.2 | 63.6 | -2.9 | 13.8 | 15.1 | 7.8 |
| 414 | 49.2 | 62.2 | -6.2 | 12.3 | 16.4 | 7.2 |
| 416 | 55.8 | 75.2 | -2.5 | 14.5 | 16.4 | 7.0 |
| 418 | 18.3 | 43.8 | -4.3 | 15.4 | 15.2 | 6.9 |
| 420 | -2.6 | 10.3 | -5.0 | 12.9 | 12.5 | 6.8 |
| 430 | -9.9 | 2.1 | -4.0 | 12.2 | 12.1 | 7.5 |
| 440 | -15.0 | -0.1 | -1.9 | 12.3 | 12.4 | 7.2 |
| 450 | -5.8 | 8.4 | -3.6 | 11.9 | 12.0 | 6.9 |
| 460 | -4.9 | 8.5 | -3.1 | 12.4 | 11.8 | 6.9 |
| 470 | -7.2 | 4.6 | -4.1 | 12.9 | 12.2 | 7.2 |
| 480 | -3.7 | 4.3 | -3.9 | 12.0 | 12.0 | 6.9 |

10 FIGURES

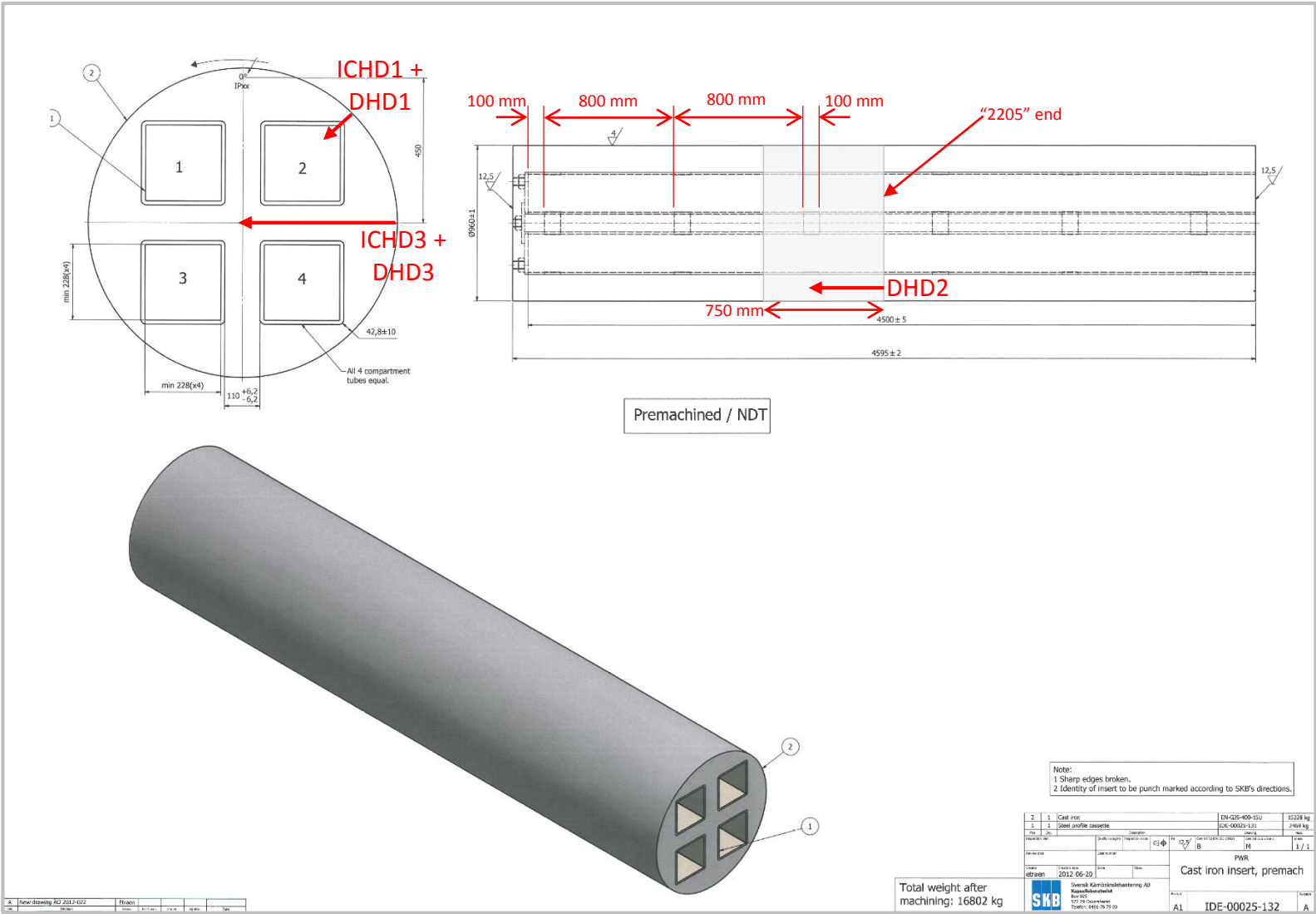


Figure 1: Technical drawing of the complete Cast Iron Insert showing the section measured by VEQTER and the location of the inserted plates at 800 mm separation. All dimensions given in mm. Annotations in red given as updates to the original CAD drawing provided to reflect the work finally carried out.

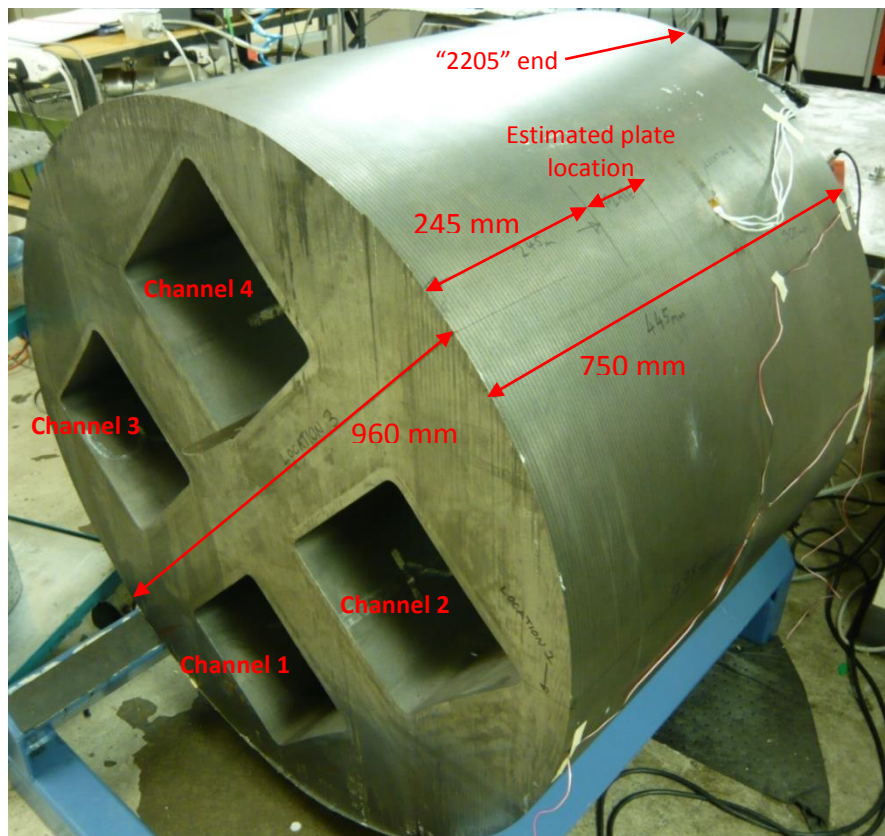


Figure 2: Photograph of the Cast Iron Insert section supplied for measurement with ICHD strain gauges attached by VEQTER.

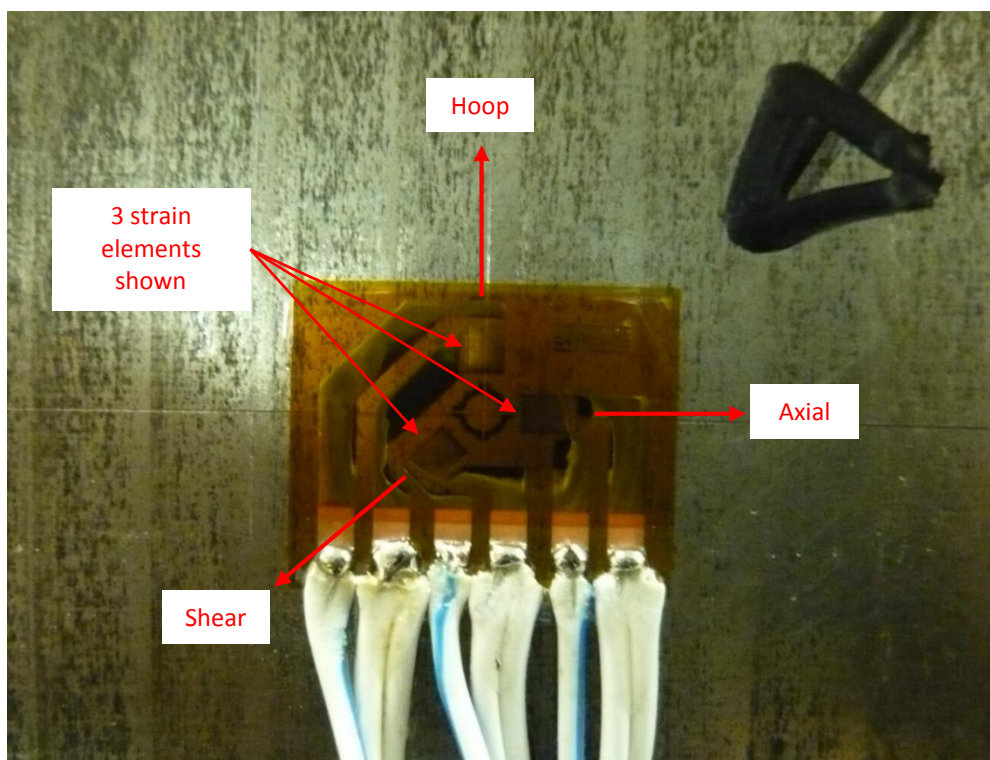


Figure 3: A photograph of the SGR attached at location ICHD3 with axes notation shown.

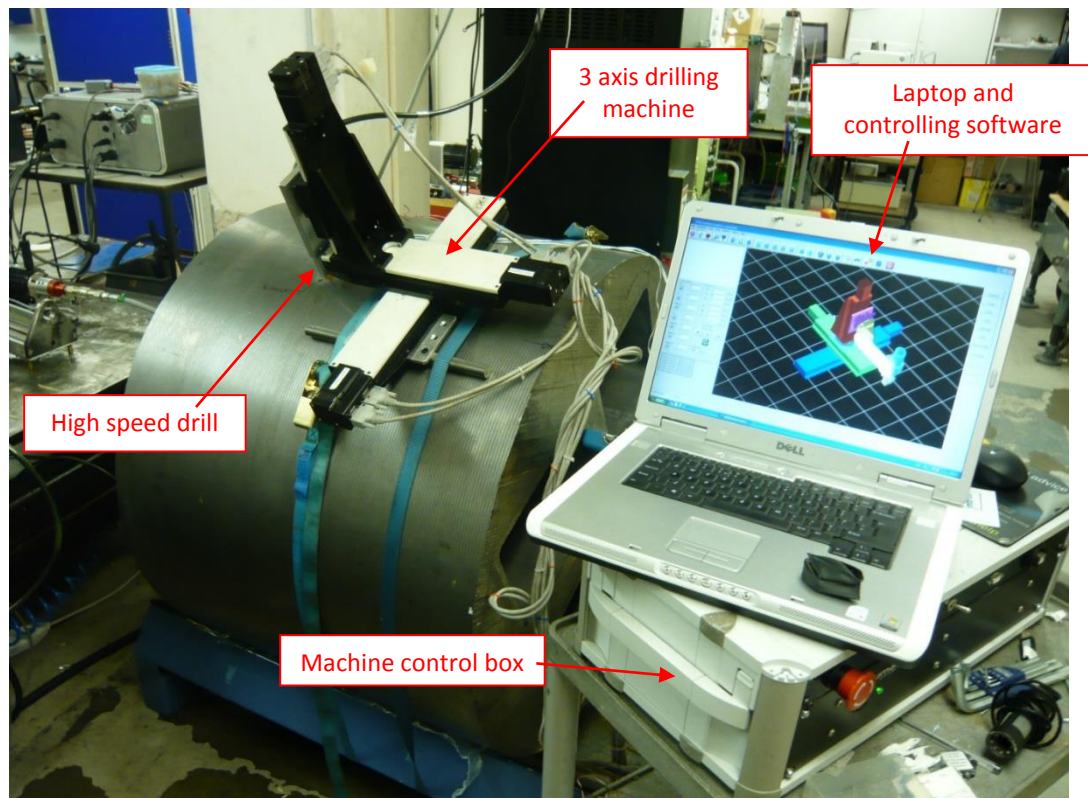


Figure 4: A photograph of the ICHD setup during the measurement process.

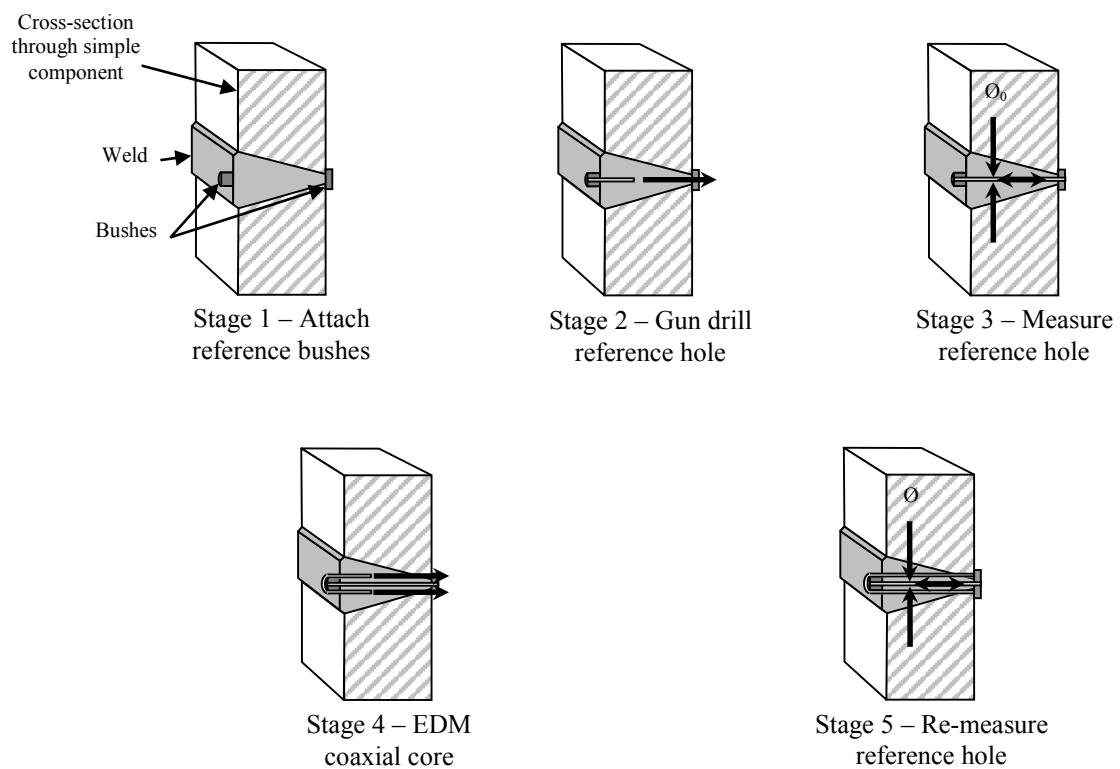


Figure 5: A schematic of the five stages involved in the standard DHD procedure for a welded component.

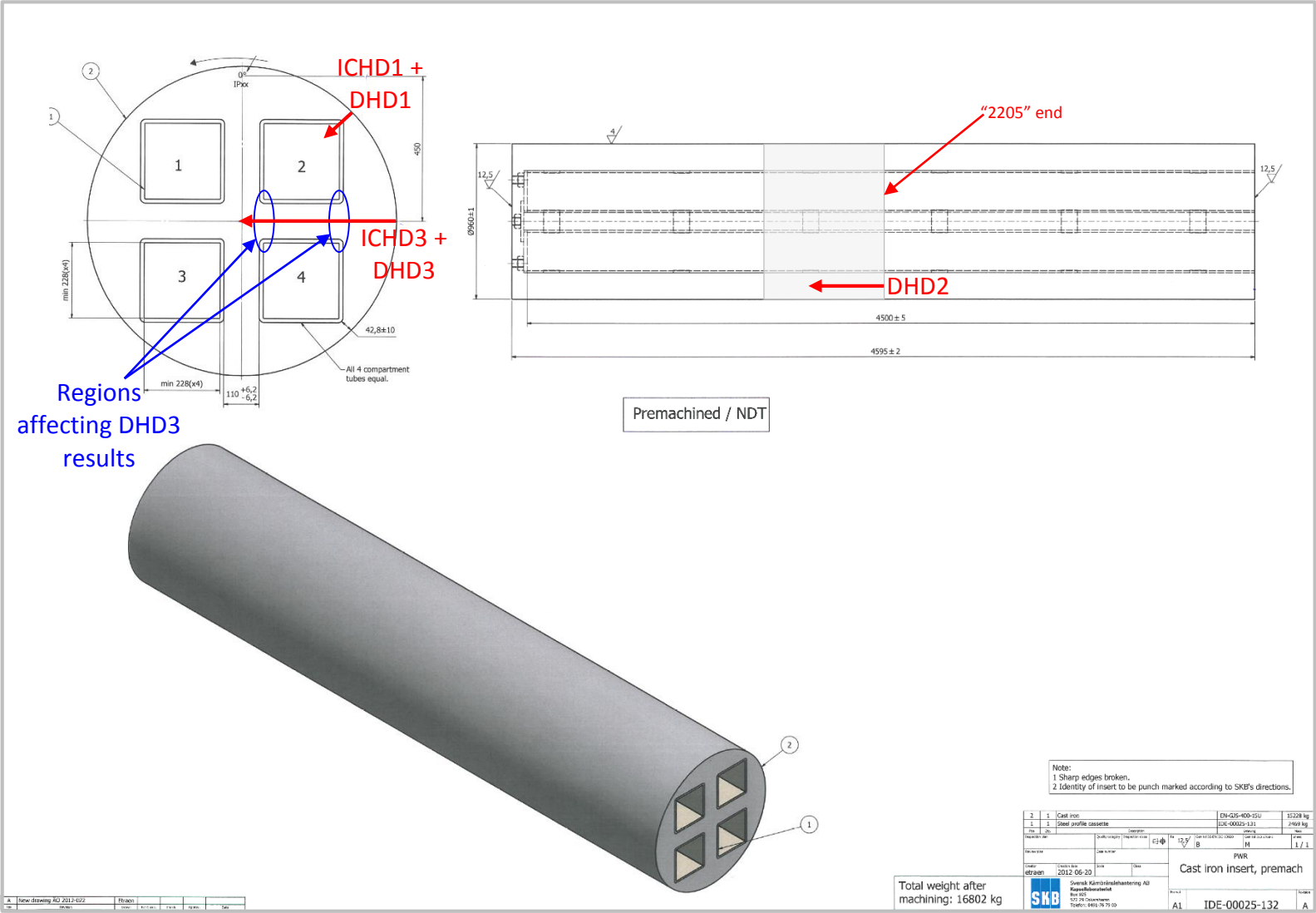
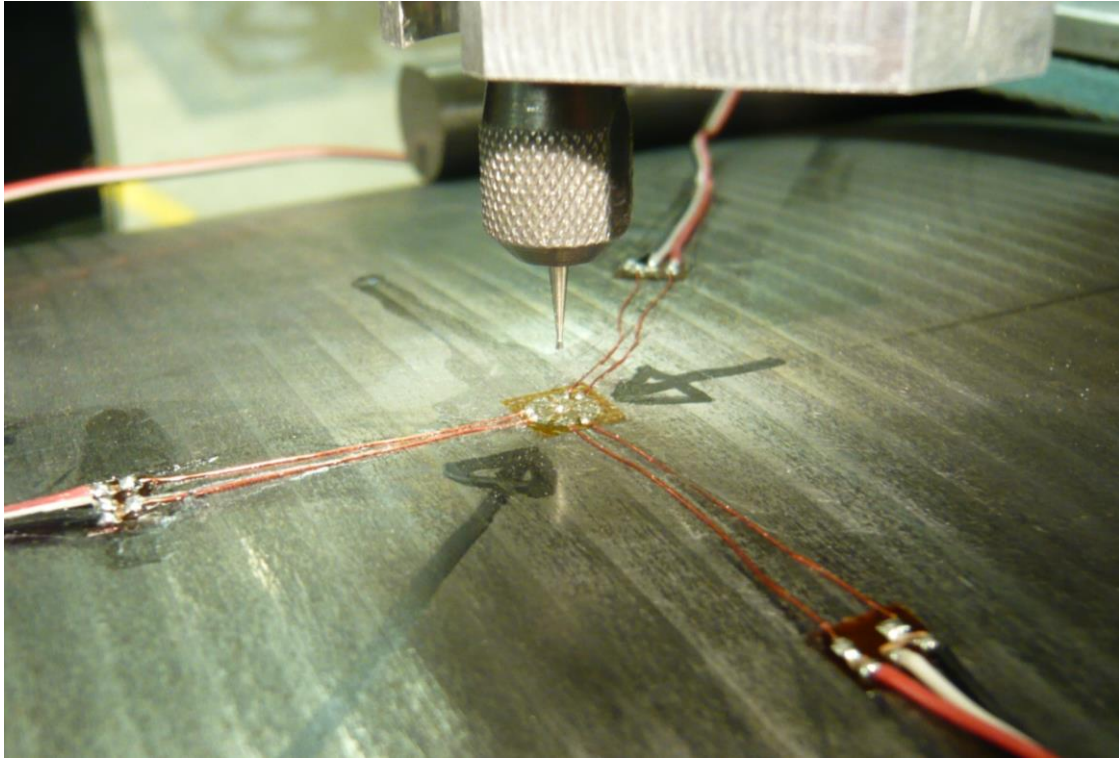
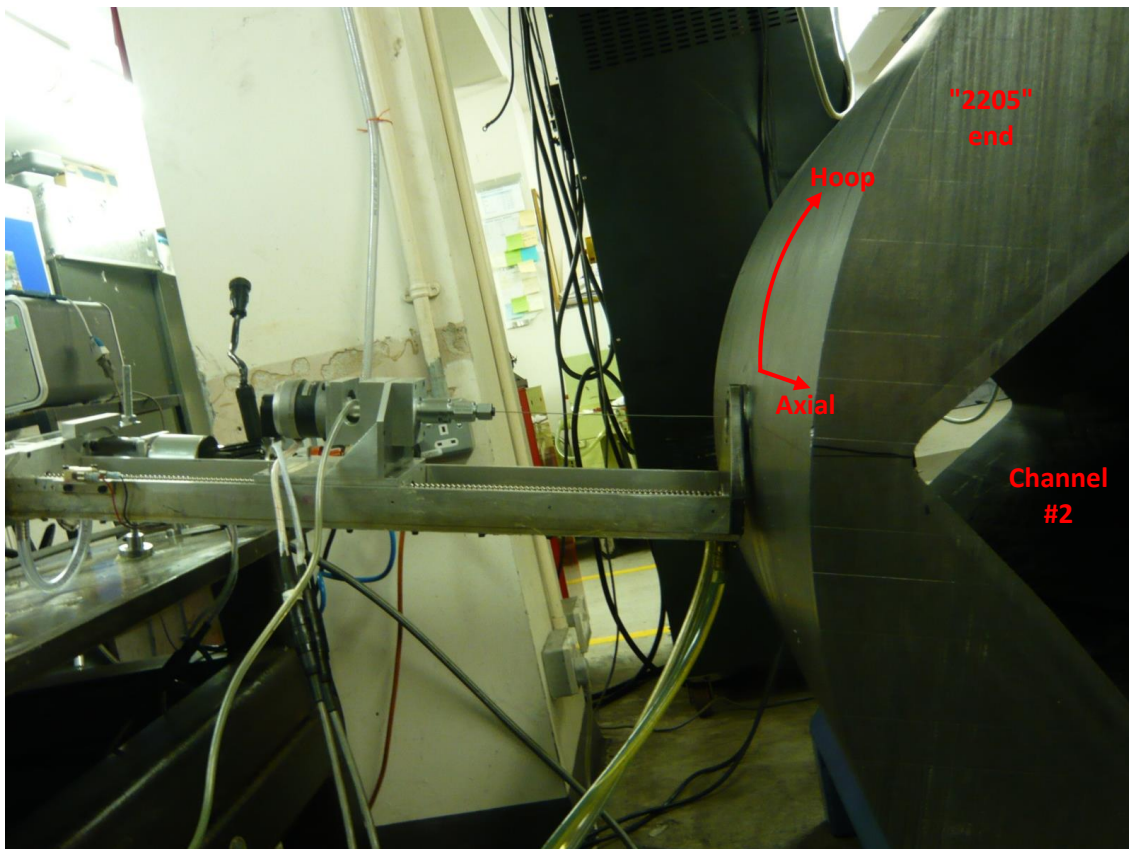


Figure 6: A technical drawing of the complete Cast Iron Insert with annotated section measured and measurement locations. All dimensions given in mm.



a) ICHD strain gauge rosette and drill set-up prior to drilling



b) DHD machine set-up during the air gauge diameter measurement of the reference hole

Figure 7: Photographs of the ICHD and DHD measurements being carried out at location 1.

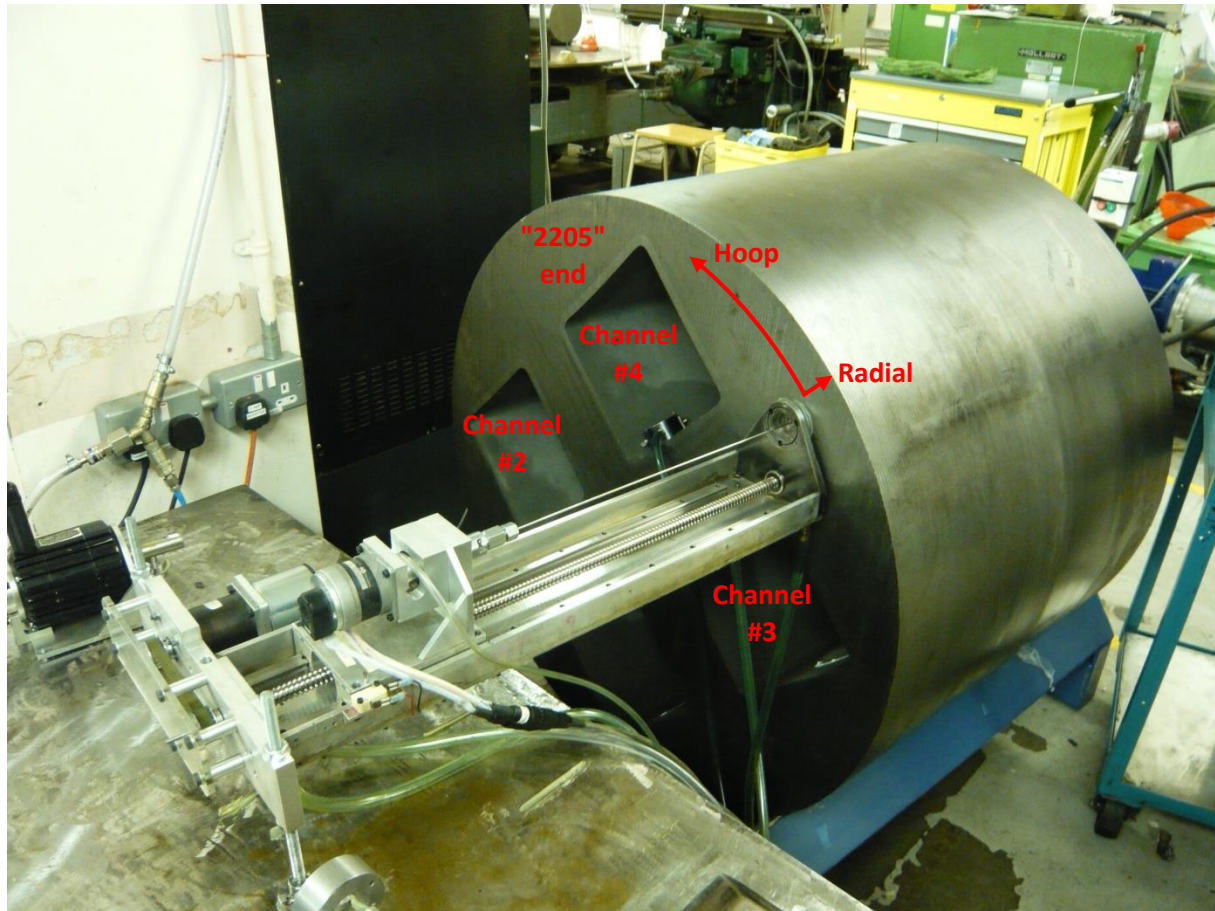
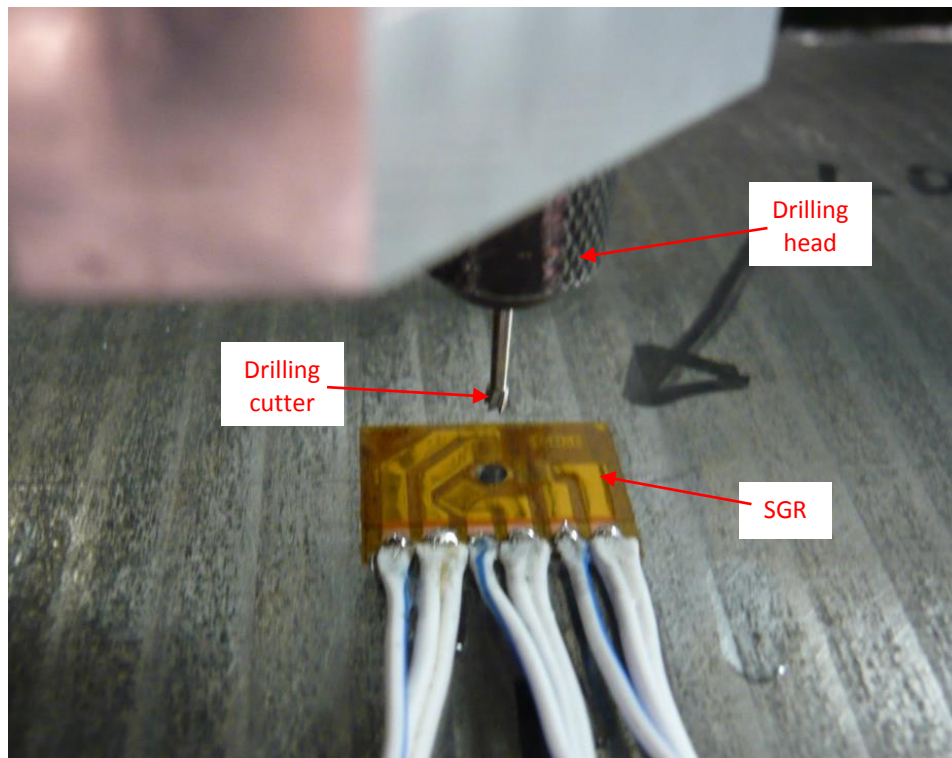
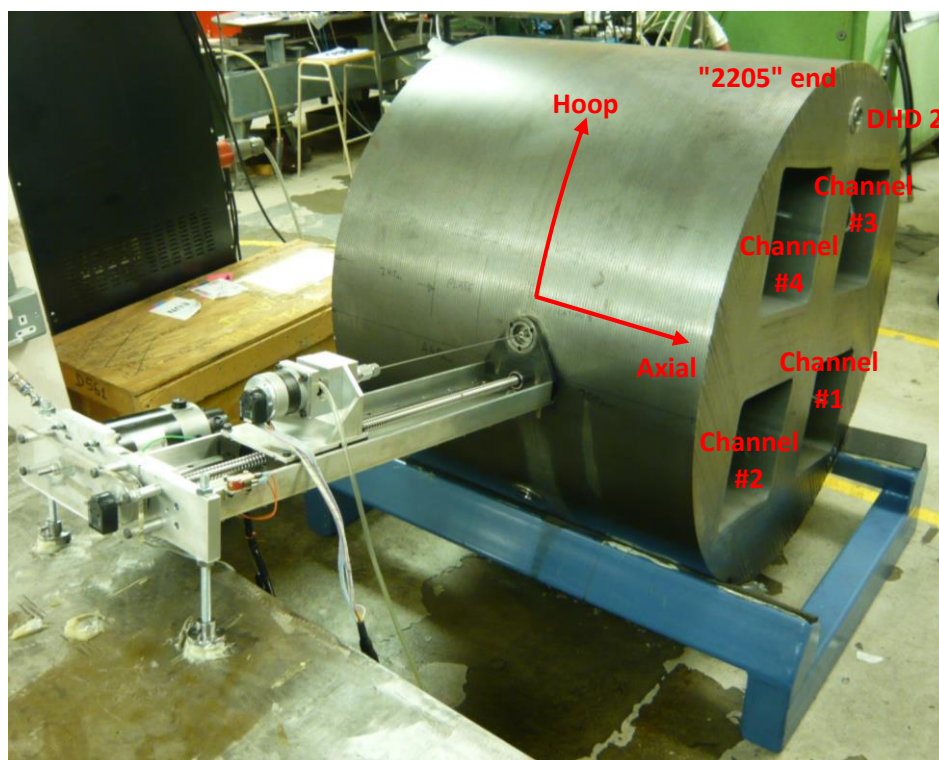


Figure 8: A photograph of the air gauge diameter measurement process being carried out at DHD2.



a) ICHD strain gauge rosette and drill set-up after drilling



b) DHD machine set-up during the air gauge diameter measurement of the reference hole

Figure 9: Photographs of the ICHD and DHD measurements being carried out at location 3.

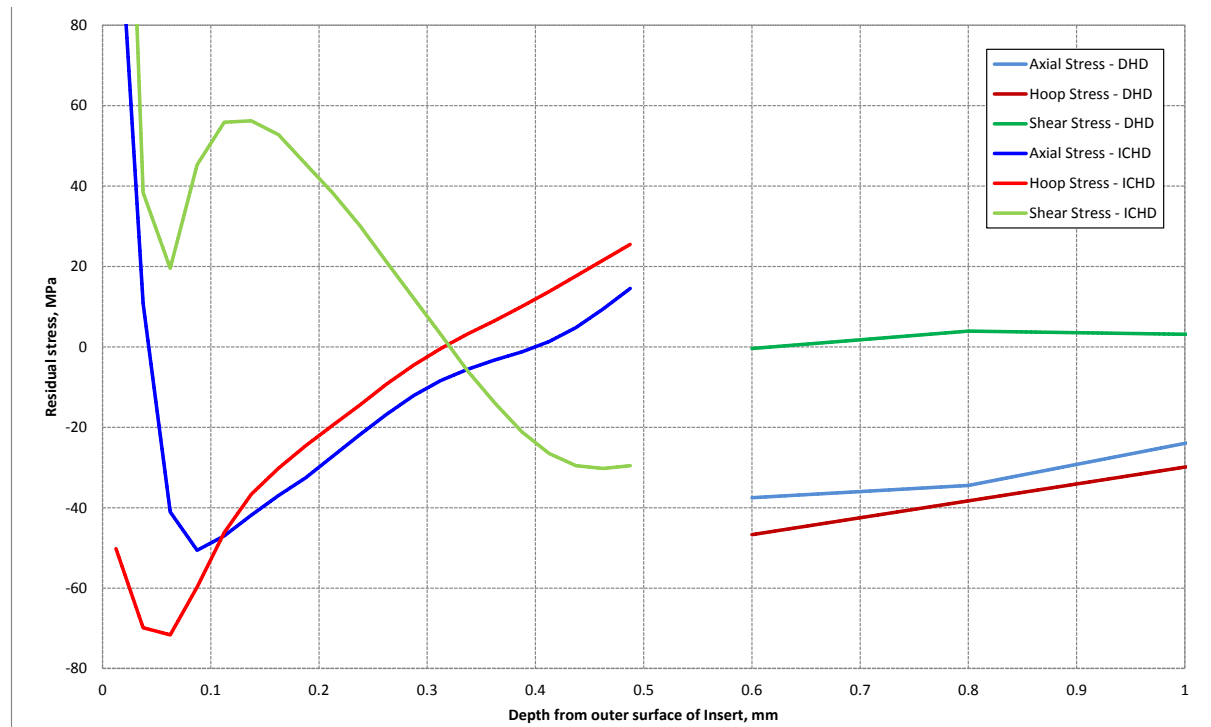


Figure 10: Residual stresses measured at the surface of location 1 (i.e. radially into the corner of channel #2 from the specimen outer diameter surface) using ICHD and DHD.

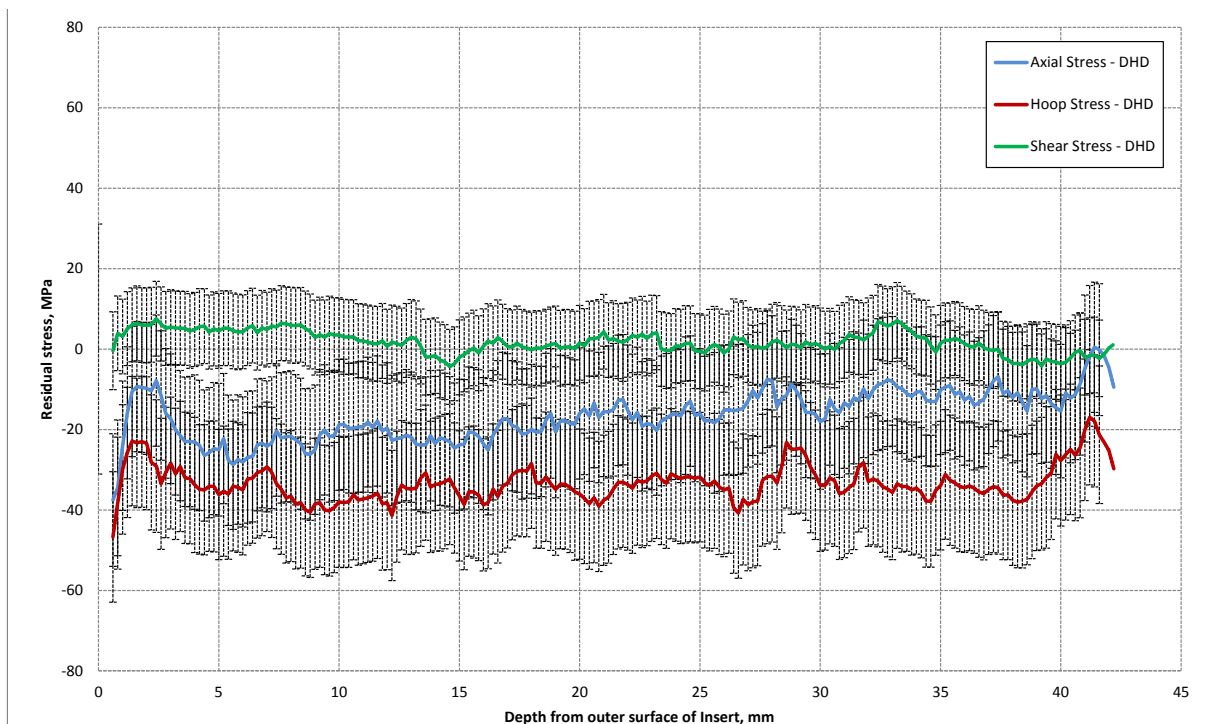


Figure 11: DHD measured residual stresses at location 1 (i.e. radially into the corner of channel #2 from the specimen outer diameter surface).

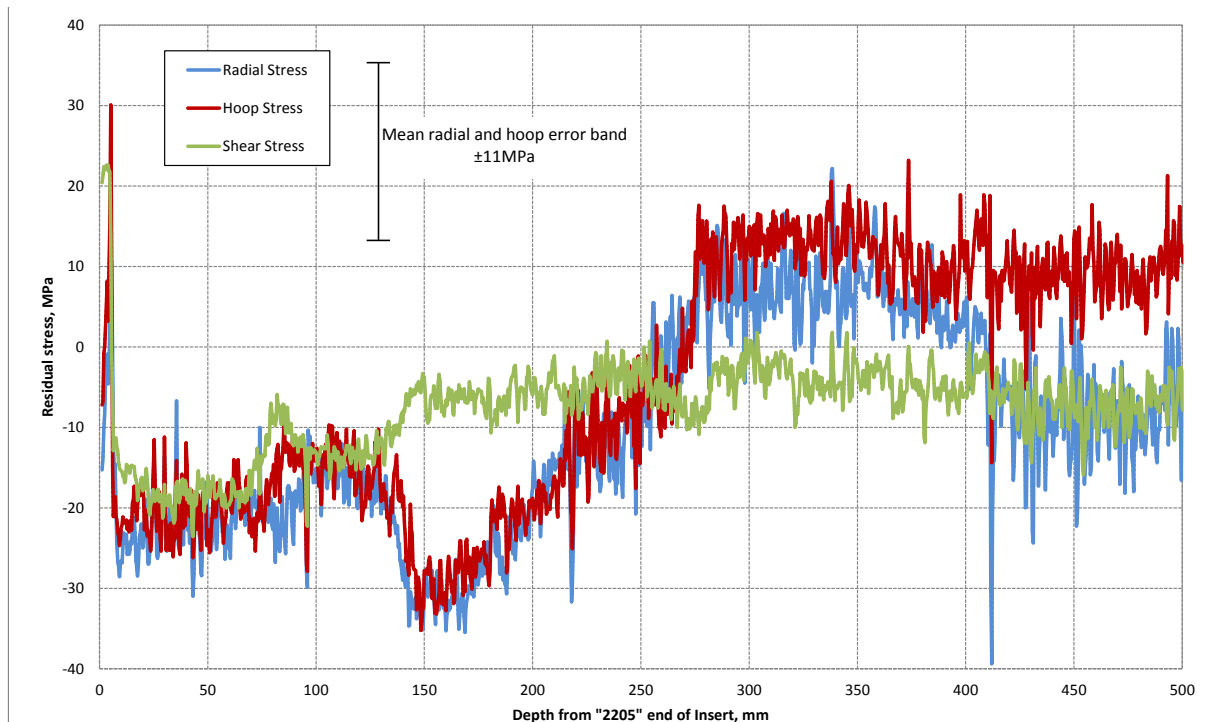


Figure 12: DHD measured residual stresses at location 2 (i.e. axially within the bulk material between channels #3 and #4, and the specimen outer diameter surface).

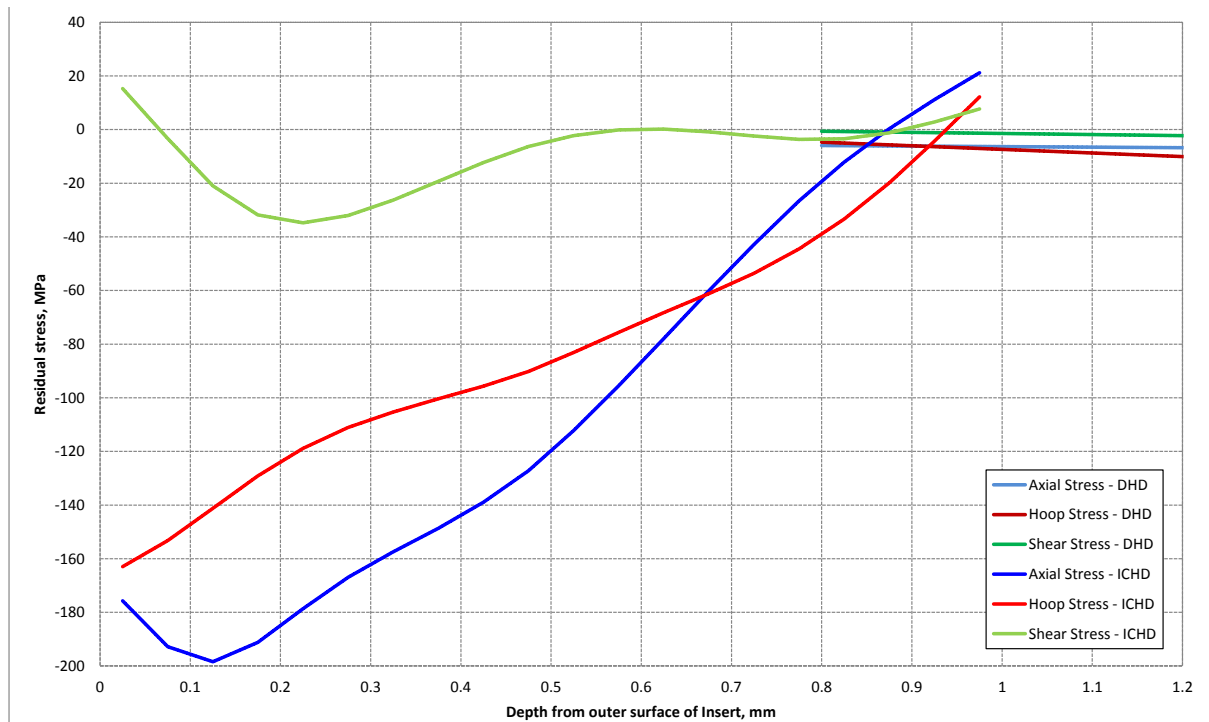


Figure 13: Residual stresses measured at the surface of location 3 (i.e. radially through the axis of the specimen from the outer diameter surface between channels #2 and #4) using ICHD and DHD.

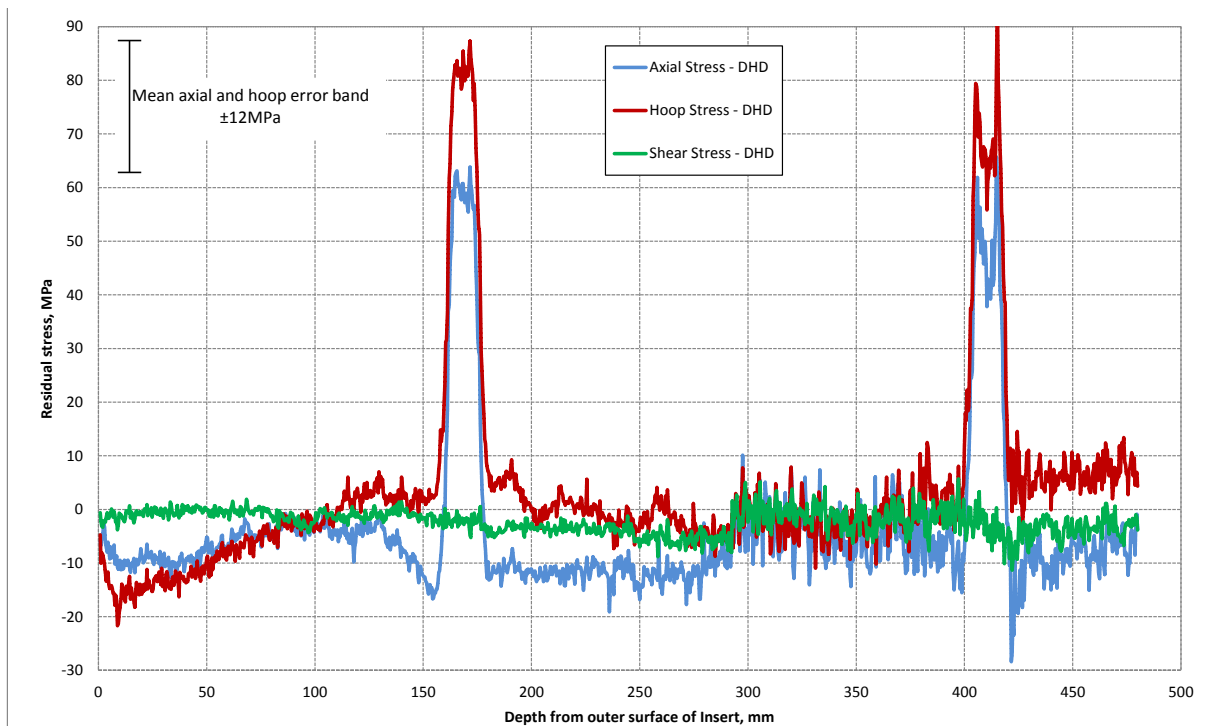


Figure 14: DHD measured residual stresses at location 3 (i.e. radially through the axis of the specimen from the outer diameter surface between channels #2 and #4).